Peak dynamic pressure on semi- and quarter- circular breakwaters under wave troughs

Xue-Lian Jiang[a, b], Qing-Ping Zou[c, 1], Ji-Ning Song [b]

[a]State Key Laboratory of Hydraulic Engineering Simulation and Safety, Tianjin University, Tianjin, China 300072

[b]Tianjin Key Laboratory of Soft Soil Characteristics & Engineering Environment, School of Civil Engineering, Tianjin Chengjian University, Tianjin, China 300384; PH (001) 22-23085076; FAX (001) 22-23085076; email: jiang.xue.lian@163.com

[c]Department of Civil and Environmental Engineering, The University of Maine, Orono, Maine 04469-5711; PH (207) 581-2178; FAX (207) 581-2113; email: qingping.zou@maine.edu

ABSTRACT: A series of tests were conducted to examine the characteristics of the wave loading exerted on circular-front breakwaters by regular waves. We found that the wave trough instead of wave crest plays a major role in the failure of submerged circular caissons due to seaward sliding. The difference in the behavior of seaward and shoreward horizontal wave forces is explained based on the variations of dynamic pressure with wave parameters. A wave load model is proposed based on a modified first-order solution for the dynamic pressure on submerged circular-front caissons under a wave trough. The prediction is accurate enough for engineering design. Further studies are needed to include model uncertainties in the reliability assessment of the breakwater.

Keywords: semicircular breakwater, quarter-circular breakwater; wave trough load, seaward wave force; shoreward wave force

1. Introduction

Caisson breakwaters are built to mitigate wave action and protect beach from erosion. Traditionally, this task has been done by a vertical wall placed on an artificial rubble mound , also known as vertical breakwaters (VB) in Goda (2010). However, with the advancement of breakwater construction sites into deeper water, a vertical breakwater is expected to experience larger wave loading, therefore, more cost due to increased concerns about the sliding and overturning failure, and the bearing capacity of foundation.

In the past decades, various breakwaters, such as sloping-top breakwaters, perforated breakwaters, and circular-front breakwaters, have been constructed in the harsh coastal

---

[1] Corresponding author. E-mail: qingping.zou@maine.edu.

environment with severe storms and poor seabed conditions. This study focuses on the circular-front caisson breakwaters including quarter-circular breakwaters (QCB) and semicircular breakwaters (SCB). As shown in Figure 1, a circular breakwater is a composite breakwater composed of a precast concrete caisson supported by a rubble mound. it acts as a rubble mound breakwater at a low water level and a composite breakwater at a high water level. In comparisons with a vertical wall, a circular wall has lesser wave load and weight so that it is more stable in the severe coastal environment (Tanimoto and Takahashi, 1994). In addition, the circular breakwaters are aesthetically pleasing, easily to construct, and economically feasible (Dhinakaran et al, 2012). QCBs have a smaller rubble mound than SCBs with the same height, therefore less expensive to build.

According to the design guidance, shoreward sliding along caisson base is the main failure mode of circular-front caisson breakwaters. The wave loading related to the shoreward sliding has been discussed by Tanimoto et al (1987), Xie (1999), Yuan & Tao (2003) for SCBs, and Xie et al. (2006) for QCBs. More details about dynamic pressures on SCBs subject to head-on waves can be found in Sundar & Ragu (1997, 1998). The effect of oblique waves on SCBs was discussed in Zhang et al (2005) and Liu & Li (2013).

Majority of previous studies of wave loading for circular-front breakwaters focus on the shoreward force due to a wave crest. In the contrary, Rao et al's (2001) and Wang's (2006) model tests showed that the seaward force may control the sliding failure of submerged SCBs.

The purpose of this paper is to develop a model to calculate the wave loads on submerged circular-front caissons due to a wave trough based on experimental data. The experimental arrangement is described in section 2. Then, the difference between the seaward and shoreward horizontal forces is investigated based on the variation of dynamic pressure with wave parameters and structure geometry in section 3. Subsequently, a wave load model for wave trough is proposed based on a first-order wave theory and validated by the measurements in section 4. Finally, some concluding remarks are summarized in section 5.

2. Experiment setup

This experiment was conducted at the State Key Laboratory of Coastal and Offshore Engineering at Dalian University of Technology. The glass-walled wave flume is 30 m long, 0.4 m wide and 0.65 m high. Waves are generated from the inlet by a piston-type

wavemaker driven by a variable-speed motor. At the outlet, a basket filled with soft materials is fixed to eliminate the reflection of waves from the downstream end of the flume.

The scale was set to 1:40 based on Froude law, geometric similarity, and the available wave conditions in the flume. Quartercircular, semicircular and vertical breakwaters were employed in the experiment. Each structure consists of a caisson and a rubble mound (see Figure 1). The caisson is impermeable made of Lead-Filled Acrylic. The height of the rubble mound (h_t) is 0.075 m, the height of the caisson (h_c) is 0.175 m, and the diameter of the quarter- and semi- circular walls is 0.15m. The bottom width of the caisson (B_c) is 0.24 m for the quartercircular and vertical sections, and 0.34 m for the semicircular section.

Seven wave gauges (G1-G7) were used to measure the variations in the free surface elevation. G1-G3 are one wavelength offshore away from the seaside of structure and used for the resolution of the incident and reflective wave. The distance between G1-G3 was adjusted immediately before each run according to the requirements of the three-probe method proposed by Mansard and Funke (1980). G4 and G5 were respectively fixed close to the front wall and the rear wall to record the wave deformation passing the caisson. G6 and G7 were set one wavelength onshore from the leeside of structure to record the transmission wave profile. The variations in the pressure on the caisson were collected by diaphragm-type transducers (P1~P19). In each run, data were recorded simultaneously from a 48-channel data acquisition card at a sampling frequency of 50 Hz.
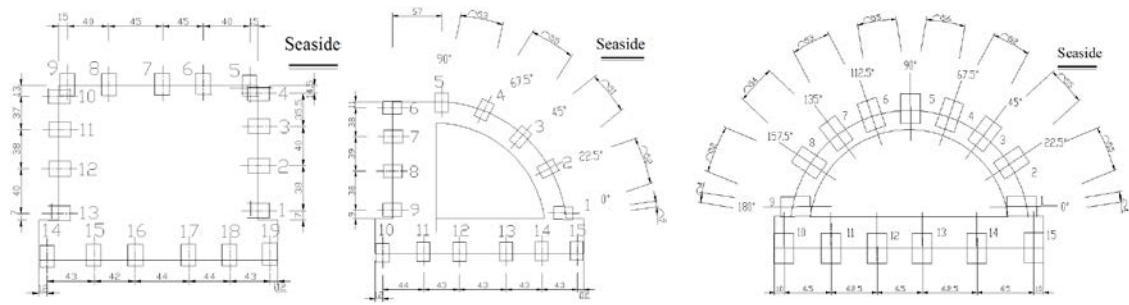
(a)
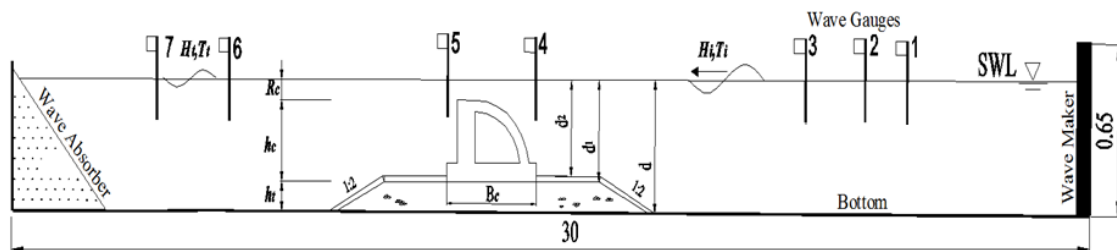
(b)

Figure 1. (a) Lateral view of experiment layout (Unit: m); (b) Configuration of pressure transducers (Unit: mm).

Three water levels (submerged, crown-level and emerged conditions), seven wave heights (0.05 m-0.11m) and six wave period (0.84s-1.20s) were used in sixteen runs (see Table 1). It should be noted that the relative freeboard height (R_c/H) varies between (-1, 1) leading to alternatively submerged-emerged case during the wave-structure interaction.

Table 1.   Wave conditions.

Water level	Depth in front of structure	Depth over rubble mound	Freeboard height	Wave height	Wave period
	d (m)	d_1 (m)	R_c (m)	H (m)	T (m)
Submerged	0.30	0.23	-0.05	0.11	1.20
	0.30	0.23	-0.05	0.09	1.20
	0.30	0.23	-0.05	0.06	1.20
	0.30	0.23	-0.05	0.11	0.96
	0.30	0.23	-0.05	0.09	0.96
	0.30	0.23	-0.05	0.06	0.96
Crown-level	0.25	0.18	0.00	0.10	1.15
	0.25	0.18	0.00	0.08	1.15
	0.25	0.18	0.00	0.06	1.15
	0.25	0.18	0.00	0.09	0.92
	0.25	0.18	0.00	0.08	0.92
	0.25	0.18	0.00	0.06	0.92
Emerged	0.20	0.13	0.05	0.07	1.08
	0.20	0.13	0.05	0.05	1.08
	0.20	0.13	0.05	0.07	0.84
	0.20	0.13	0.05	0.05	0.84

In the following discussion, dynamic pressure (p) is positive towards the structure, horizontal force (F_h) is positive shoreward, the vertical (F_v) and uplift forces (F_u) are positive upwards. It should be noted that the vertical force is the sum of the uplift force applied to the caisson base and the vertical pressure component exerted on the caisson walls.

3. Results analysis

3.1. Experiment verification

Figure 2 (a) compares the prediction by the second-order Stokes theory and measured wave profile in the calibration test. It shows the wave conditions in table 1 were well reproduced in the wave flume. Figure 2 (b) demonstrates that the measured dimensionless maximum horizontal force is consistent with the observations of Wang (2006) for the SCB.
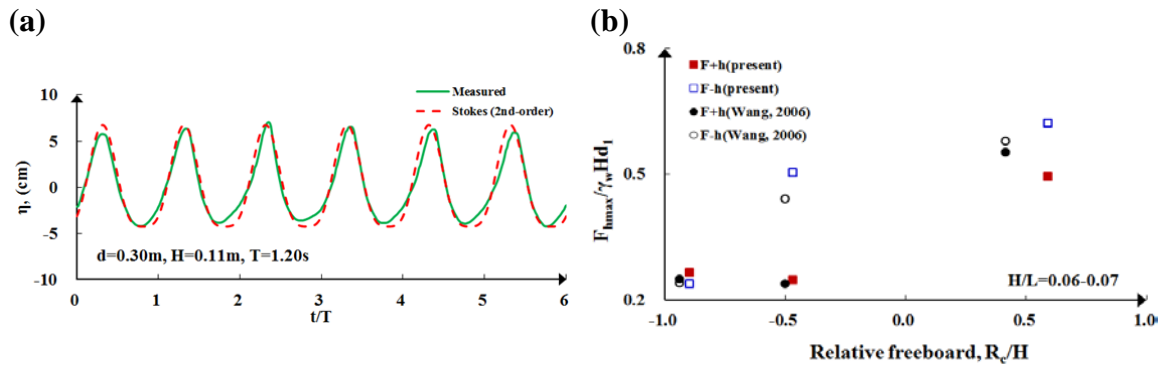

Figure 2. Comparison of (a) the measured and predicted wave profiles, (b) the dimensionless maximum horizontal force from the present and previous experiment for SCB.

3.2. Components of wave loading

Figure 3 shows the typical time series of the force components for submerged vertical and quarter-circular breakwaters. The sliding force is calculated from the expression $F_{slide} = F_h + f \cdot F_v \cdot sign(F_h)$, where $f = 0.6$ is the friction coefficient between caisson and rubble mound. It shows the vertical breakwater has a larger peak horizontal force than the circular-front breakwaters due to stronger reflection by the plain upright wall. In addition, the horizontal force has a greater phase shift form the vertical force but a smaller phase shift from the uplift force. At larger submergence, the peak seaward horizontal force becomes larger and its phase is approaching to that of the peak upward vertical force. As a result, the peak sliding force tends to arise at the time of the maximum seaward horizontal force. The instantaneous surface elevation indicates that a high wave trough generally causes the maximum seaward horizontal force.

For the non-emerged condition (including submerged and crown-level cases), our analysis shows that the occurrence frequency of the maximum sliding force at the time of the maximum seaward horizontal force $F_{-h\max}$ is 42% for the vertical breakwater, 92% for the quarter-circular breakwater, and 75% for the semicircular breakwater. The

results suggest that the instability of non-emerged circular-front breakwaters caused by sliding more likely occurs when a wave trough instead of a wave crest pass the front wall. This conclusion is consistent with Rao et al (2001) and Wang (2006) but in contrary with the recommendation of existing design criteria for QCB and SCB.
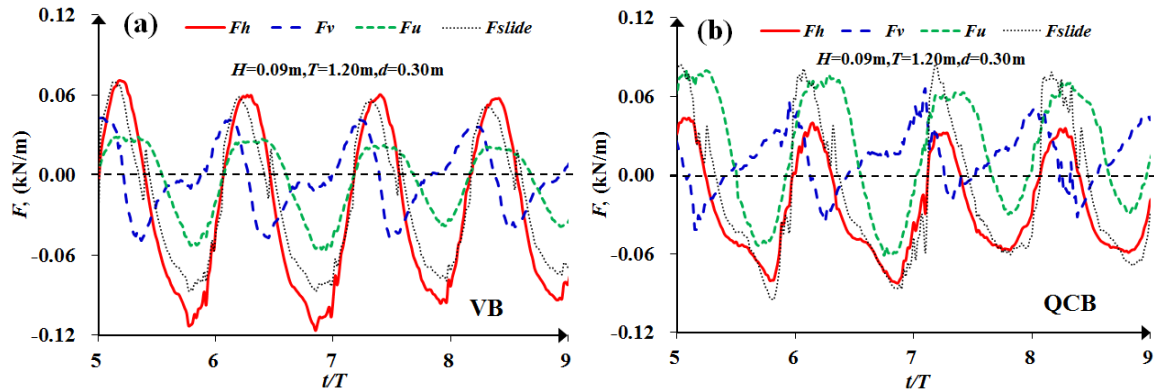

Figure 3. Time series of the horizontal force (F_h), vertical (F_v) and uplift force (F_u) and sliding force (F_{slide}) for relative freeboard height R_c/H =-0.606: (a) vertical breakwater; (b) quarter-circular breakwater.

Xie et al (2006) reported that a quartercircular breakwater has an up to 30% larger horizontal force than a semicircular breakwater by a wave crest in the submerged case. Jiang et al (2008) caught a strong trailing vortex clinging to the rear wall of a submerged quartercircular by a RANS model as a wave crest is passing over the caisson. This large-scale turbulent eddy might cause an extra downstream force on a submerged quartercircular. However, under the wave trough, the maximum seaward horizontal force in this experiment for non-emerged semi- and quarter- circular breakwaters gives a mean ratio of 1.0 and a standard deviation of 0.1. To examine the mechanism behind these phenomena, we compared the numerical results of flow field around both QCB and SCB breakwaters under a wave trough in Figure 4. Both structures have the same undulation in the wave profile focusing near the front face. Although a stronger trailing vortex is formed on the leeside of the quarter-circular caisson, it is away from the rear wall and hence leads to a small impact on the dynamic pressure exerted on the structure.
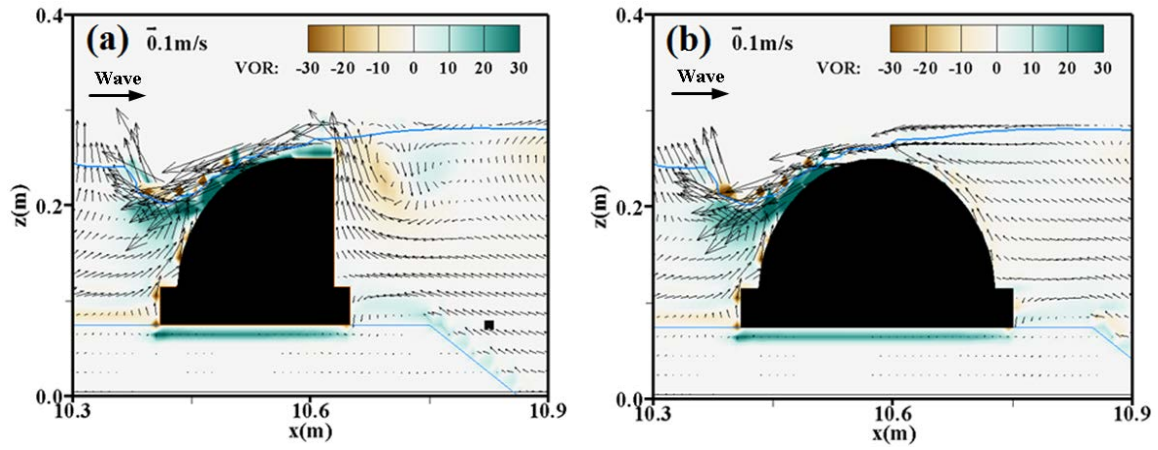
Figure 4. Velocity and vorticity fields under a wave trough around (a) quarter-circular breakwater; (b) semicircular breakwater. (H=0.11 m , T=1.20 s , d=0.30 m , R_c/H =-0.468).

3.3. Variation of wave loading with wave and structure parameters

This section will further explore the reason why the non-emerged circular-front breakwaters have a greater horizontal force in seaward direction than shoreward direction. Jiang et al. (2012) concluded that the hydrodynamics of head-on waves interacting with circular breakwaters are significantly affected by relative freeboard, wave steepness and relative wave height. Therefore, we will discuss the effects of these three parameters on wave force.

3.3.1. Variation of wave force with relative freeboard

Figure 5 indicates that for submerged circular breakwaters ($R_c/H \leq 0$), the seaward horizontal force has a greater magnitude than the shoreward horizontal force while they are close to each other in the emerged case ($R_c/H > 0$). Herein, the horizontal force is normalized by $\gamma_w H h_p$, where γ_w is the specific weight of seawater; h_p is the action range of wave pressure on the caisson ($h_p = h_c$ for submerged breakwater and $h_p = d_1$ for emerged breakwater).
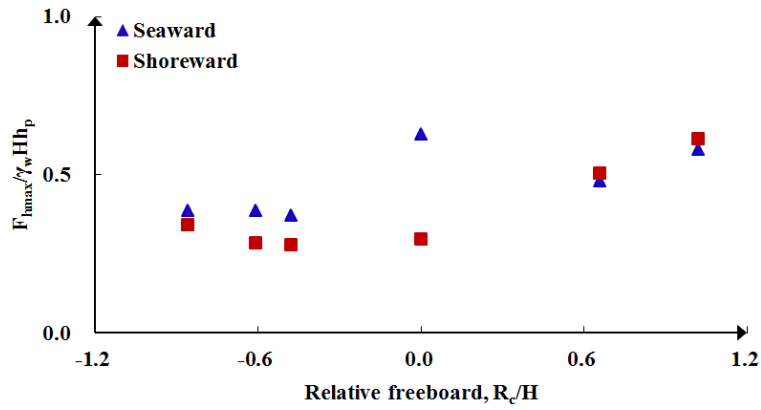
Figure 5. Variation of the dimensionless horizontal force with the relative freeboard.

We use the instantaneous pressure distribution to explain Figure 5 (see Figure 6). It shows that the pressure on the front wall contributes most to the peak horizontal force when a wave crest or a wave trough arrives at the toe of caisson. Comparison of Figure 6 (a) and (b) indicates that the pressure by the wave trough is larger at the lower part of the front wall. For a curved wall, the pressure exerted on the lower part undergoes a smaller reduction than that on the upper part due to lesser phase shift from wave crest or wave trough. In addition, the angle between the directions of the pressure on the lower part and the horizontal line is smaller than that on the upper part. As a result, the horizontal component of the pressures under a wave trough is greater than that under a wave crest.
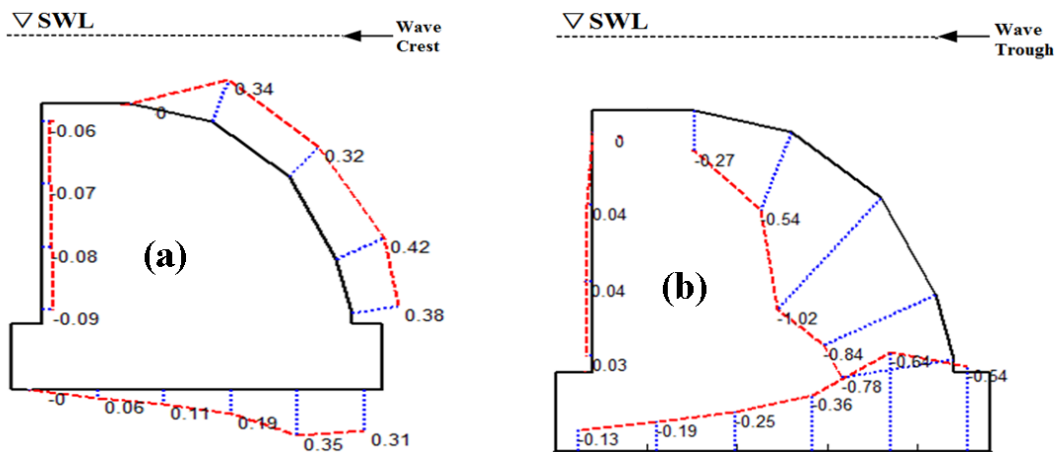

Figure 6. Instantaneous pressure distribution for the submerged quarter-circular breakwater where relative freeboard height R_c/H =-0.468. (H =0.11 m, T =1.20 s, d =0.30 m; Unit: kPa).

3.3.2. Variation of wave force with wave steepness

Figure 7 shows that the peak shoreward and seaward horizontal forces increase with decreasing wave steepness and the variation in the peak seaward horizontal force is relatively smaller.
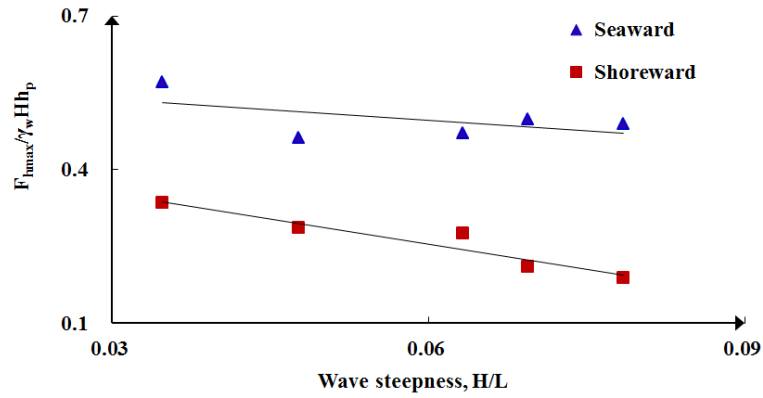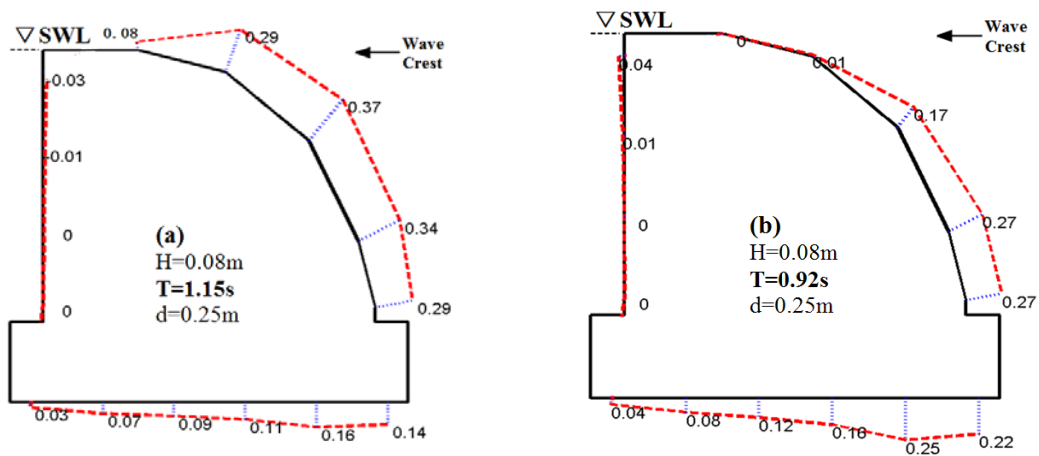

Figure 7. The dimensionless horizontal force versus the wave steepness for the quarter-circular breakwater when relative freeboard height R_c/H =0.

Figure 8 gives the instantaneous pressure distribution due to waves with a same wave height but different periods at the crown water level. At the phase of wave crest, the longer wave strengthens the pressure on the front wall considerably than the shorter wave (see Figure 8 (a) and (b)). At the phase of wave trough, the pressure distribution focuses more on the lower part of the front wall and presents a small change with the wavelength (see Figure 8 (c) and (d)). Therefore, the peak shoreward horizontal force is more sensitive to the variation in the wavelength than the seaward horizontal force, as shown in Figure 7.
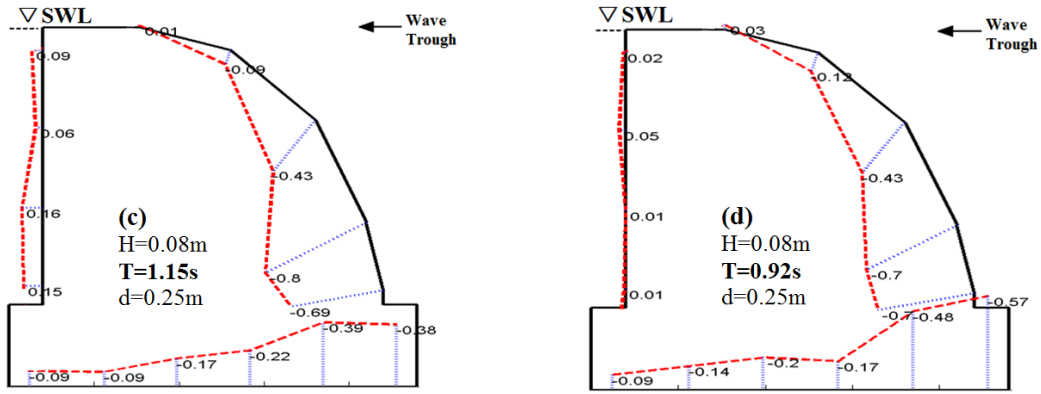
Figure 8. Instantaneous pressure distribution for different wavelengths when relative freeboard height R_c/H =0. (Unit: kPa).

3.3.3. Variation of wave force with relative wave height

Figure 9 demonstrates that the peak seaward horizontal force increases with the relative wave height at a faster rate than the peak shoreward horizontal force in the non-emerged case. Herein, the horizontal force is normalized by $\gamma_w L h_p$, where L is the local wavelength at the toe of structure.
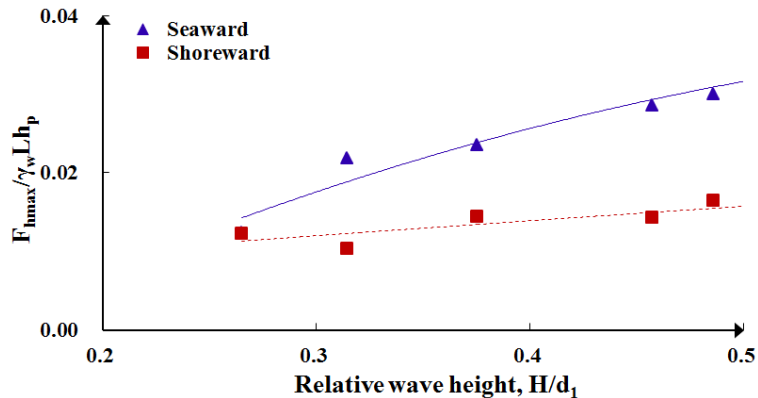

Figure 9. The dimensionless horizontal force versus the relative wave height for the quarter-circular breakwater where freeboard height R_c =-0.052 and 0.

Figure 10 presents the instantaneous pressure distribution due to waves with a same wave period but different wave heights. From Figure 10 (a) and (b), under the wave crest, the pressure exerted on the upper part of the front wall increases faster with wave height than that exerted on the lower part. This leads to a smaller increase in the shoreward horizontal force due to a greater phase shift and central angle at the upper part of the curved wall. On the contrary, under the wave trough, the pressure on the lower part of the front wall increases at a faster rate with wave height and therefore leads to a greater increase in the seaward horizontal force (see Figure 10 (c) and (d)).

This implies a greater impact of wave height on the peak seaward horizontal force than on the peak shoreward horizontal force.
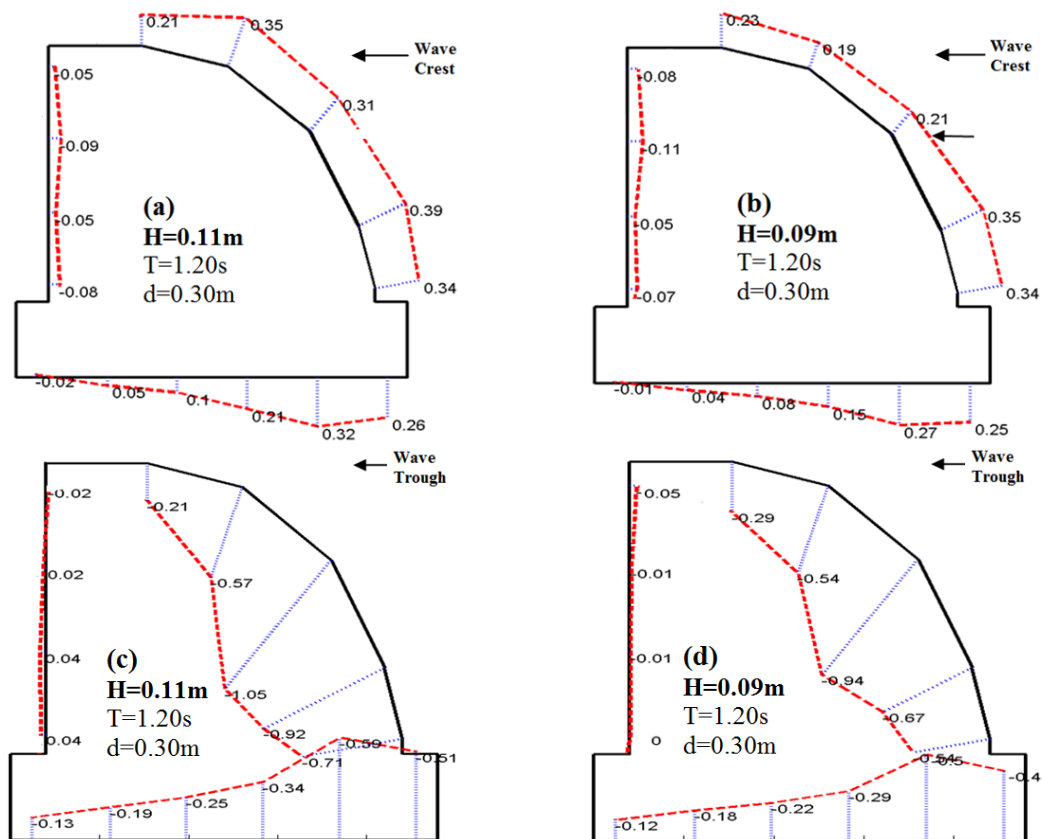

Figure 10. Instantaneous pressure distribution under wave crest (Upper) and wave trough (Lower) for wave heights of 0.11 m (Left) and 0.09 m (Right) when freeboard R_c=-0.052. (Unit: kPa).

4. Wave load model under wave trough

The foregoing discussion suggests that the pressure under the wave trough more likely dictates the stability of a submerged circular-front caisson against seaward sliding. However, the existing models focus on the wave loads under the wave crest Only Rao et al (2001) and Wang (2006) proposed the empirical formulas to calculate the wave loads under wave trough for SCBs. Yet these formulas were obtained based on the regression analysis of a set of specific measurements so that their applicability is restricted.

Until now, first or higher order wave theories have been the basis for regular wave loading exerted on breakwaters. For example, the first order wave theory has been developed for standing waves by Boussinesq (1872) in deep water and by Sainflou (1928) in shallow water. The second order theory has been developed by Miche (1944), Biesel (1952), Rundgren (1958), Penney & Price (1952), and the third order wave theory by Tadjbaksh and Keller (1960). Goda (1967) obtained the fourth order pressure

solution of the finite amplitude standing wave on a vertical wall. Li (1990) noted that a modified first order approximation based on experimental data often yields a better prediction than a higher order theory, despite that the latter is more rigorous. Therefore, the present study will develop a wave load model for pressures on a submerged circular-front caisson under wave trough based on the first order solution.

First order approximation of pressure for the standing wave in front of a vertical wall by Sainflou (1928) is employed in this study. As pointed out by Qiu (1986), Sainflou's model is valid for d/L=0.1-0.2 and $H/L \geq 1/30$, therefore the wave conditions in table 1.

The surface elevation in the Sainflou's model is given by

$$
\begin{aligned}
\eta = z &+ \frac{H \sinh k(d+z)}{\sinh kd} \sin kx \sin \omega t \\
&+ \frac{1}{2} kH^2 \frac{\cosh k(d+z) \sinh k(d+z)}{\sinh^2 kd} \cos 2kx \sin^2 \omega t
\end{aligned}
\tag{1}
$$

The third term on the right hand side of Eq. (1) is nonperiodic that leads to a vertical shift in the mean displacement of free surface during a wave period

$$
h_s = \pi H^2 \coth kd / L
\tag{2}
$$

The wave-induced pressure can be calculated by

$$
p(z) = \gamma_w H \left[\frac{\cosh k(d+z)}{\cosh kd} - \frac{\sinh k(d+z)}{\sinh kd} \right] \sin kx \sin \omega t
\tag{3}
$$

where $k = 2\pi/L$ is the incident wave number, $\omega = 2\pi/T$ the incident angular wave frequency, x the horizontal coordinate with x=0 at the toe of front wall and positive toward the structure, z the vertical coordinate with z=0 at the still water level and positive upward.

As discussed above, the seaward horizontal force reaches its peak value when a wave trough arrives at the toe of the caisson. Obviously, the wave-induced pressure at a location downstream from the toe of the circular wall is smaller than that at the vertical face of the breakwater due to phase shift. Xie (1999) proposed a phase modification coefficient $\lambda_p = \cos(k\Delta x)$ for submerged SCBs based on the small amplitude wave theory, where Δx is the horizontal distance between the action point of pressure and the toe of caisson. Tanimoto & Kimura (1985) and Takahashi & Hosoyamada (1994) presented the phase modification coefficients for impermeable inclined walls and sloping-top caissons, respectively. Tanimoto et al (1987) suggested an empirical coefficient $\lambda_p = \cos^4(k\Delta x)$ for emerged SCBs. These recommendations have been

tested in this study and the best agreement between the prediction and the measurement is reached using $\lambda_p = \cos^4(k\Delta x)$. Substituting this coefficient into Eq. (3), we obtain the pressure after the phase adjustment

$$p'(z) = \lambda_p p(z), \qquad \lambda_p = \cos^4(k\Delta x). \tag{4}$$

The uplift pressure exerted on the bottom of caisson is assumed to follow a triangular distribution with zero heel pressure and toe pressure given below:

$$p_u = p_b = p(z = d_1). \tag{5}$$

Figure 11 illustrated the procedure (from right to left) of estimating the wave loads on a submerged circular-front caisson by the modified first-order theory. Following the procedure, the total force exerted on the caisson can be calculated by

$$F_h = \int_{\widehat{AB}} p'(z)\cos\theta\, dl, \quad F_v = \int_{\square}^{\square} p'(z)\sin\theta\, dl + 0.5 p_u B_c, \quad F_u = 0.5 p_u B_c. \tag{6}$$
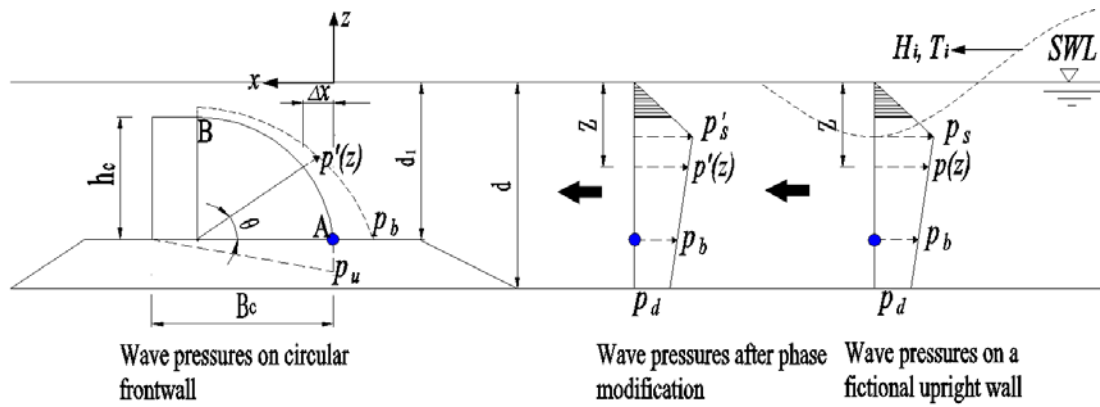

Figure 11. The procedure of calculating wave pressures exerted on a circular-front wall (in the order of from right to left).

The predictions by the modified first order theory are compared with the measurements in Figure 12. From Figure 12 (a), the mean ratio of predicted to measured pressures P-1 to P-4 by wave trough varies between 0.85 and 1.05 that indicates a reasonable theory and data agreement. From Figure 12 (b), the ratio of prediction to measurement for the peak seaward horizontal force is 0.93 for the QCB, 0.96 for the SCB, and 0.91 for the VB. The corresponding standard deviation is 0.22 for the QCB, 0.19 for the SCB, and 0.10 for the VB. For an emerged vertical wall, McConnell (2000) noted that the ratio of Sainflou model's prediction to measurement follows a Gaussian distribution, whose mean value and standard deviation are 0.89 and 0.15, respectively. His statistical parameters are close to those of the present study for the VB. In addition, the ratio of prediction to measurement for the uplift force is 1.07 for the QCB, 1.18 for the SCB,

and 1.06 for the VB. The corresponding standard deviation is 0.18 for the QCB, 0.17 for the SCB, and 0.21 for the VB.
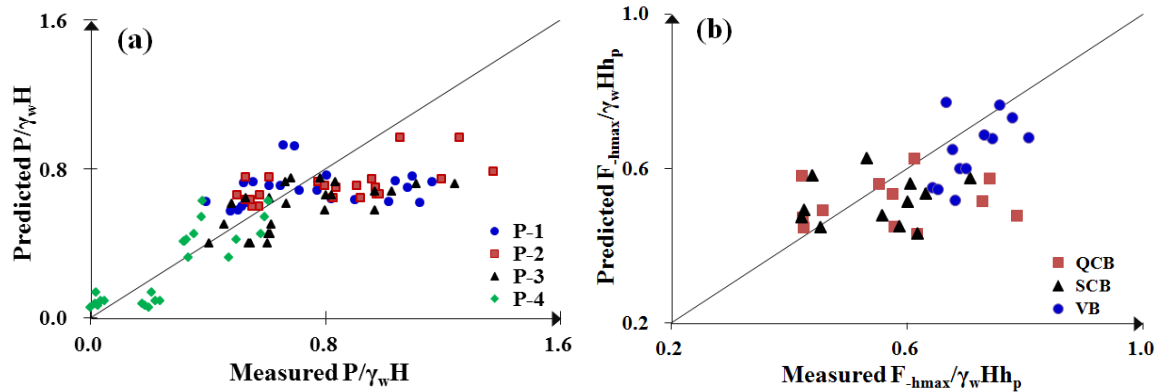

Figure 12. Comparison of the predicted and measured (a) pressures on submerged quarter- and semi- circular breakwaters under wave trough and (b) peak seaward horizontal forces for submerged quartercircular, semicircular, and vertical breakwaters under wave trough. P-1~P-4 represents the recordings by the No.1~No.4 pressure transducers.

5. Conclusions

The horizontal wave force exerted on a circular-front breakwater reaches its peak value when a wave crest or a wave trough arrives at the toe of caisson. In the submerged case, the peak seaward horizontal force increases with the relative wave height at a faster rate than the peak shoreward horizontal force, therefore, wave trough instead of wave crest plays a dominant role in the stability of circular-front breakwaters against seaward sliding

Wavelength has a lesser while wave height has a greater impact on the peak seaward horizontal force than on the peak shoreward horizontal force.

The modified first order wave theory with a phase adjustment is sufficiently accurate for predicting the pressures and the peak seaward horizontal force on a submerged circular-front caisson subject to wave trough. It should be noted that this model is applicable with the limitation of $-1.0 \leq R_c/H \leq 1.0$, $d/L = 0.1$-0.2 and $H/L \geq 1/30$, where R_c the freeboard height, H the wave height, d the depth in front of structure and L the wave length.

One of the largest uncertainties in the prediction is due to the structure geometry. Therefore, before applying this model to design circular-front breakwaters, a reliability-based study needs to be done to identify suitable partial safety factors to account for the associated uncertainties.

6.   Acknowledgments

7.   References

Biesel, F., 1952. Equations generales au second ordre de la houle irreguliere, *Houille Blanche*, **5**: 372-376.

Boussinesq, J., 1872. Théorie des ondes et des remous qui se propagent le long d'un canal rectangulaire horizontal, en communiquant au liquide contenu dans ce canal des vitesses sensiblement pareilles de la surface au fond, *Journal de Mathématiques Pures et Appliquées. Deuxième Série* **17**: 55-108.

Dhinakaran, G., Sundar, V. and Sundaravadivelu, R., 2012. Review of the research on emerged and submerged semicircular breakwaters, *Proceedings of the Institution of Mechanical Engineers, Part M: Journal of Engineering for the Maritime Environment*, **226**(4): 397-409.

Goda, Y. and Kakizaki, S., 1967. Study on finite amplitude standing waves and their pressures upon a vertical wall, *Coastal Engineering in Japan* **10**: 1-11.

Goda, Y., 2010. *Random Seas and Design of Maritime Structures*, 3rd Edition, Singapore, World Scientific.

Jiang, X.L., Gu, H.B. and Li, Y.B., 2008. Numerical simulation on hydraulic performances of quarter circular breakwater, *China Ocean Eng.,* **22**(4): 585-594.

Jiang, X.L.，Guo, S.L. and Li, Y.B., 2012. Study on hydraulics and wave energy dissipation as wave passing circular breakwater, *The Ocean Engineering*, **30(3)**: 59-67.

Li, Y. C., 1990. *Wave action on marine structures*, 1st Edition, Beijing, China, The Ocean Publishing Company: 1-50.

Liu, Y. and Li, H. J., 2013. Analysis of oblique wave interaction with a submerged perforated semicircular breakwater, *J. Eng. Math,* **83**: 23-36.

Mansard, E.P.D. and Funke, E.R., 1980. The measurement of incident and reflected spectra using a least square method, *Proc. of the 17th ICCE, ASCE* **1**: 154-172.

McConnell, K. J., Allsop, N. W. H. and Flohr, H., 1999. Seaward wave loading on vertical coastal structures, *Proc. Int. Conf. Coastal Structures'99*, Santander, Spain: 447-454.

Miche, R., 1944. Mowvements Ondulatoires de la mer in Profondeur Constante on Decroissante, *Annals des Ponts el Chaussees*, Paris: 121, 3.

Penney, W. G. and Price, A. T., 1952. Finite periodic stationary gravity waves in a perfect liquid, *Phil. Trans. Roy. Soc., ser, A.*, **244:** 254-284.

Qiu, D. H., 1986. *Wave theory and its application in Engineering*, 1st Edition, Beijing, China, High Education Press. (In Chinese)

Rao, Y.H., Yu, Y.X. and Zhang, N.C., 2001. Hydraulic experimental study on submerged semicircular breakwaters, *ACTA OCEANOLOGICA SINICA,* **23**(2): 124-131. (In Chinese)

Rundgren, L., 1958. Water wave forces: a theoretical and laboratory study, *Bulletin of the Division of Hydraulics at the Royal Institute of Technology*, Stockholm, Sweden, Kungl. Tekniska Högskolan, **54**.

Sainflou, G., 1928. Essai sur les digues maritimes verticales, *Ann. Ponts et Chaussees,* **98**(11): 5-48.

Sundar, V. and Ragu, D., 1997. Wave induced pressures on semicircular breakwaters, *2nd Indian national conference on harbour and ocean engineering*, Thiruvananthapuram, Kerala, India: 278-287.

Sundar, V. and Ragu, D., 1998. Dynamic pressures and run-up on semicircular breakwaters due to random waves, *Ocean Eng.,* **25**(2-3): 221-241.

Tadjbakhsh, I. and Keller, J. B., 1960. Standing surface waves of finite amplitude, *Journal of Fluid Mechanic,* **8**: 442-451.

Takahashi, S., and Hosoyamada, S., 1994. Hydrodynamic Characteristics of Sloping Top Caissons. *Proceedings of International Conference on Hydro-Technical Engineering for Port and Harbour Construction*, Port and Harbour Research Institute, Japan, **1**: 733-746.

Tanimoto, K., Yoshinoto, N., Namerikawa, N. and Ishimaru, Y., 1987. Hydraulic characteristics and design wave forces of semi-circular caisson breakwaters, *Coastal Engineering, JSCE*, **34**: 551-555.

Tanimoto, K., and Kimura, K., 1985. A Hydraulic Experimental Study on Trapezoidal Caisson Breakwaters, *Technical Note No. 528*, Port and Harbour Research Institute, Yokosuka, Japan. (In Japanese)

Tanimoto, K. and Takahashi, S., 1994. Japanese experience on composite breakwaters, *International workshop on wave barriers in deep waters*, Yokosuka, Japan, Nagase, Port and Harbor Research Institute: 1-24.

Wang, L.Q., 2006. *The study of 2-d and 3-d random waves acting on a semicircular breakwater*, Doctoral Dissertation, Dalian University of Technology.

Xie, S.L., 1999. Wave forces on submerged semicircular breakwater and similar structures, *China Ocean Eng.,* **13**(11): 63-72.

Xie, S.L., Li, Y.B., Wu, Y.Q. and Gu, H.B., 2006. Preliminary research on wave forces on quarter circular breakwater, *The Ocean Engineering*, **24**(1): 14-18. (In Chinese)

Yuan, D.K. and Tao, J.H., 2003. Wave forces on submerged, alternately submerged, emerged semicircular breakwater, *Coast. Eng.,* **48**(2): 75-93.

Zhang, N. C., Wang, L.Q. and Yu, Y.X., 2005. Oblique irregular waves load on semicircular breakwater, *Coast. Eng. J.,* 47(4): 183-204.